Open Access

OBM Genetics

LIDSEN Publishing Inc.

Original Research

Anti-cancer Drug Susceptibility of Breast Cancer Cells Incubated on Electrospun Polymeric Fiber Substrates

Rie Sasaki [‡], Hiroto Ito, Masami Okamoto [*]

Advanced Polymeric Nanostructured Materials Engineering, Graduate School of Engineering, Toyota Technological Institute, 2-12-1 Hisakata, Tempaku, Nagoya 468 8511 Japan; E-Mails: r-sasaki@menicon.co.jp; sd19405@toyota-ti.ac.jp; okamoto@toyota-ti.ac.jp

‡ Current Affiliation: Basic Research Department, Central R&D Lab, 5-1-10 Takamoridal, Kasugai, 487-0032 Japan

* **Correspondence:** Masami Okamoto; E-Mail: okamoto@toyota-ti.ac.jp

Academic Editor: Vidhula Ahire

Special Issue: Tumor Micro-environment and Metastasis in Solid Tumors

OBM Genetics
2022, volume 6, issue 2
doi:10.21926/obm.genet.2202155

Received: March 01, 2022
Accepted: June 05, 2022
Published: June 14, 2022

Abstract

In this study, we examined the effect of a combination of surface topographies (fiber alignments) and different stiffness of poly(L-lactic acid) (PLLA) substrates on the direct relationship between anti-cancer drug (CDDP) sensitivity for MDA-MB-231 cells and mesenchymal properties under both normal and hypoxic conditions. In addition, we studied the induction of epithelial–mesenchymal transition (EMT). The CDDP treatment under hypoxia indicated poor adhesion of MDA-MB-231 cells as well as significant repression of E-cadherin (CDH1). The robust connection between drug sensitivity and repression of epithelial cell marker of E-cadherin (CDH1) mediated by substrate surface topography contributed to the anti-cancer drug resistance of MDA-MB-231 cells. PLLA substrates did not cause a significant change in the induction and acquisition of EMT, indicating that EMT exerted no effect on drug susceptibility.

Keywords
Cancer cells; epithelial–mesenchymal transition; drug sensitivity; cell cycle; substrate surface topography

1. Introduction

Breast cancer is one of the most common female malignancies in Japan; its prevalence is attributed to poor treatment outcomes owing to resistance to radiation and chemotherapy [1-3]. The primary cause of death in patients with breast cancer is metastasis to distant organs [4]. During cancer progression, cancer cells destroy the balanced and normal state of the tumor microenvironment. These disruptions induce the expression of several genes, unregulated proliferation of cells, and migration, thus, promoting cancer malignancy [5]. In addition, cancer cells lead to the development of an abnormal extracellular matrix (ECM). In addition, cancerous cells remodel the ECM and provide biochemical and biophysical cues to adjacent cells (e.g., cancer cells and stromal cells) to accelerate cancer progression [6-9].

Despite the extensive repertoire of available therapies and ongoing efforts to incorporate new drugs into clinical practice, it is still difficult to control cancer. The application of several drugs used to treat cancer is limited by their inability to reach the site of metastasis; thus, their effectiveness remains questionable. This is especially noticeable in patients with metastatic solid tumors who are often resistant to first-line chemotherapy; thus, this approach is only palliative and frequently leads to disease progression and eventual death. Therefore, there exists a lack of a clear understanding of how cancer cells evolve to ensure survival and promote metastasis.

Cancer cells receive mechanical signals (clues) from aberrant ECMs by generating traction forces that affect their fate [10, 11]. Therefore, new platforms (or cancer models) are required to explore promising cancer therapies and predict the potential for cancer metastasis, cell proliferation, and drug sensitivity. In this context, a few studies have reported the effect of different substrate stiffness on the drug susceptibility of cancer cells [12-17].

These previous studies reported that hard substrates tend to increase drug resistance in cancer cells. However, a single factor in substrate hardening is highly simplistic to the local microenvironment conditions, making it difficult to prove effective in the drug susceptibility of cancer cells. In addition, recently proposed hypotheses have suggested that EMT plays a crucial role in cancer metastasis, recurrence, and drug susceptibility [18].

The tumor microenvironment can induce EMT. The ability of metastatic cancer to shift the mode of movement by EMT is one of the primary features of infiltration. In this respect, the relationship between drug susceptibility and EMT has received considerable attention. However, there exists a lack of a comprehensive analysis of the role of EMT in regulating drug susceptibility of breast cancer cells. Previous studies have demonstrated that artificial ECMs that combine both different surface topography (fiber arrangements) and different stiffness of polymer substrates can mimic the *in vivo* microenvironment [19].

Artificial nanofiber scaffolds can induce EMT in certain breast and lung cancer cells [19]. We have previously reported [20] the effect of a combination of surface topographies (fiber alignments) and different stiffness of the polymeric substrates on cellular morphology,

proliferation, motility, and gene expression regarding EMT in two different types of breast cancer cells (MDA-MB-231 and MCF-7).

In this study, we examined the effect of polymer substrate surface topography and stiffness on the direct relationship between drug susceptibility and mesenchymal properties of cancer cells under both normal and hypoxic conditions. We believe that understanding the link between drug sensitivity and EMT biology of breast cancer cells will provide new solutions for the development of novel therapeutic strategies.

2. Materials and Methods

2.1 Materials and Electrospinning

Poly(L-lactic acid) (PLLA)(D content = 0.8%, M_w = 102 kDa, M_w/M_n = 2.71 [20]) was used as previously described [21]. Cisplatin, [*cis*-diammine-dichloroplatinum(II)] (CDDP), an anti-cancer drug (Supplementary materials), was purchased from Tokyo Chemical Ind. Ltd. Electrospinning was conducted according to the procedure described in our published literature [21]. As control of electrospun fiber substrates, spin-coated substrates were used. All substrates were coated with 2% gelatin (Sigma-Aldrich) to enhance cell adhesion. The details have been described in our previous study [21].

2.2 Cell Culture

Human breast cell line, MDA-MB-231 (ATCC), was cultured in high glucose Dulbecco's modified Eagle's medium (DMEM) (Nacalai Tesque, Japan) supplemented with 10% (v/v) fetal bovine serum (FBS), 100 unit/mL penicillin (Nacalai Tesque), and 100 μg/mL streptomycin (Nacalai Tesque), grown at 37°C under 5% CO_2 atmosphere and 95% relative humidity (normoxia) or hypoxic condition (94% N_2, 5% CO_2 and 1% O_2) at 37 °C. Cells were grown to 70 to 80% confluence at normal culture conditions before being seeded onto fiber substrates.

2.3 Drug Susceptibility

The detailed protocol to study drug susceptibility has been described in our previous study [21]. For PLLA and PCL substrates, MDA-MB-231 cells were seeded at a density of 5.0×10^3 cells cm^{-2} on spin-coated flat substrates (designated as F-), random fibers (designated as R-), and aligned fibers (designated as A-) substrates and incubated for 3 days under both normoxic and hypoxic conditions at 37 °C and subsequent drug treatments were performed to evaluate drug sensitivity. The anti-cancer drug (CDDP) was diluted with a complete culture medium (DMEM) and added to each well. The concentrations used for this work ranged from 0 to 50.0 μM. After additional incubation for 3 days with each drug under both normoxia and hypoxia at 37 °C, the cell viability was assessed by the WST-8 assay (Dojindo) according to the manufacturer's instructions. The half-maximal inhibitory concentration (IC_{50}) values were estimated from the dose–response curves.

2.4 Flow Cytometry

MDA-MB-231 cells were seeded onto each substrate cultured under normoxic and/or hypoxic conditions at a density of 2.0×10^4 cells cm^{-2} for 6 days with or without subsequent drug

treatment of CDDP at a concentration equal to IC_{50} for each culture condition for 3 days. After incubation, cells were washed twice with cold phosphate-buffered saline (PBS) and collected by trypsin treatment. The cells were then washed, centrifuged again twice in PBS, and fixed overnight at 4 °C with 10 mL of 100% MeOH. Afterward, cells were centrifuged and washed twice with 10 mL of PBS for 30 min and propidium iodide (PI, Sigma-Aldrich) solution (PBS containing 0.25 mg/mL RNAse, pH 7.4, 37 °C) [22]. It was further resuspended in 50 µg/mL PI for 30 min in the dark at room temperature. Cell cycle distribution was analyzed by flow cytometry (Attune NxT Acoustic Focusing Cytometer, Thermo Fisher Scientific). Data analysis was performed using the FlowJo v.10.0 Software. The details of real time polymerase chain reaction (RT-PCR) have been described in our previous study [23].

2.5 Statistics

All data presented are expressed as the mean and standard deviations (±SD). Statistical analysis was performed using a one-way analysis of variance with Tukey–Kramer' *post-hoc* testing, and the significance was considered at a probability of $p < 0.05$ [23].

3. Results and Discussion

3.1 Electrospun Polymeric Nanofibers

Figure S2 shows the morphology of the resulting randomly and/or aligned electrospinning polymeric fibers [21]. As revealed by field emission-scanning electron microscope (FE-SEM) observations, all electrospun fibers have a uniform, bead-free, smooth surface morphology with an average fiber diameter of approximately 1.5 µm. Table S1 summarizes the properties of these fiber substrates obtained from FE-SEM micrographs, tensile tests, and differential scanning calorimetry. The average fiber diameter of A-PLLA and R-PLLA fibers was approximately 1.5 µm. The tensile properties of aligned fibers exhibit significantly stronger than those of random electrospinning fibers.

3.2 Drug Susceptibility

MDA-MB-231 cells were incubated with different concentrations ranging from 3.1 to 50.0 µM of CDDP molecules on day 3 under both normoxic and hypoxic conditions (Figure 1). The WST-8 assay to detect living cells showed that with concentrations up to 50.0 µM, a significant reduction in the vitality occurred in comparison with the control (0 µM) [21]. The IC_{50} values of three different types of substrates under different oxygen concentration levels estimated from sigmoidal curves (Figure 1) are presented in Figure 2. Interestingly, MDA-MB-231 cells showed different IC_{50} values when cultured on different substrates. Under normoxic conditions, cells on A-PLLA exhibited a higher resistance against CDDP compared with other substrates (1.9-fold higher for R-PLLA). The IC_{50} values were compared under both normoxic and hypoxic conditions. The IC_{50} values of cells incubated on each substrate were more affected by the hypoxic condition. Almost three-fold higher resistance was observed for MDA-MB-231 cells under hypoxia after incubation on A-PLLA when compared to that on incubation on R-PLLA under normoxia. Cellular drug resistance appeared to be affected by a combination of substrate stiffness and topography under different oxygen concentration levels.

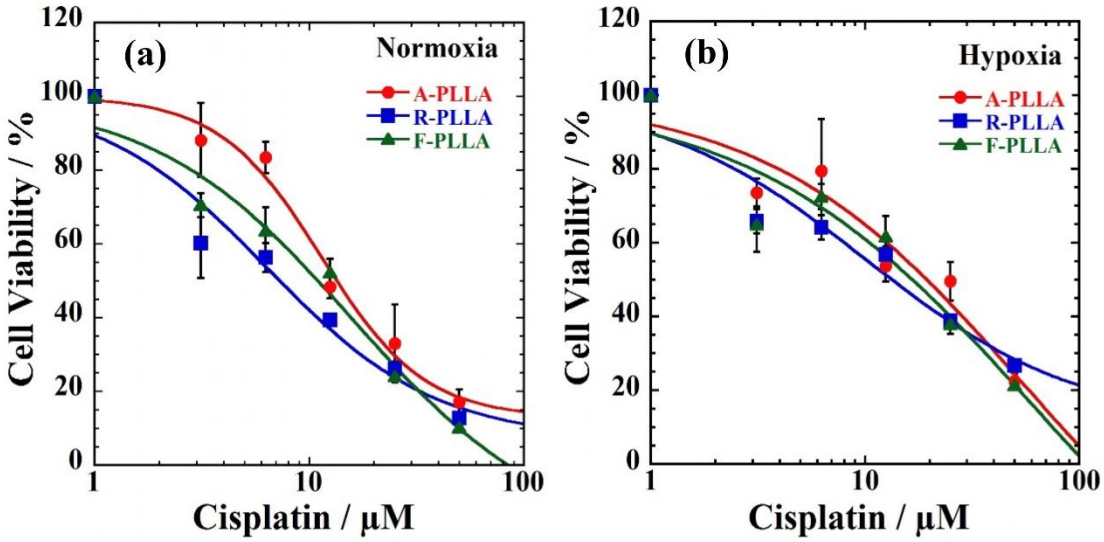

Figure 1 Cell viability as measured by the WST-8 assay using MDA-MB-231 cells treated with different concentrations of CDDP on three different PLLA substrates under (a) normoxic and (b) hypoxic conditions. Results are expressed as mean ±SD (standard deviation) (n = 5).

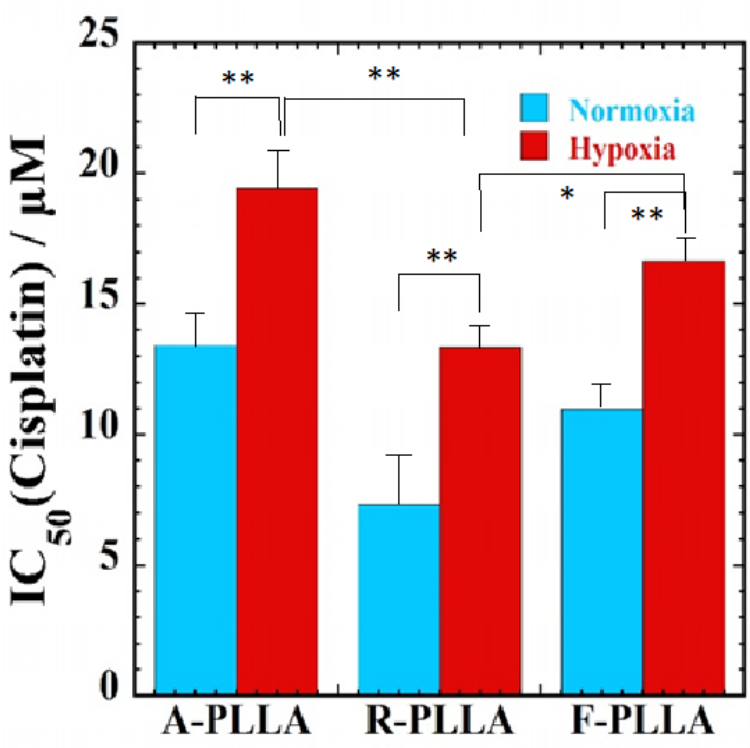

Figure 2 IC_{50} of MDA-MB-231 cells cultured on three different (A-, R-, F-) PLLA substrates treated with CDDP under both normoxic and hypoxic conditions. *p < 0.05 and **p < 0.01.

3.3 Cell Cycle Arrest of MDA-MB-231 Cells Cultured on Substrates

To better understand the proliferation state of cells, the cell cycle distribution was studied (Figure 3). As discussed in our previous study [22], cell proliferation is controlled by different phases such as the G_0/G_1 (containing two copies of each chromosome), S (synthesis of chromosomal DNA), and G_2/M (doubled chromosomal DNA) phases. Under both normoxia and hypoxia, MDA-MB-231 cells cultured on each PLLA substrate exhibited a notable difference in the distribution from days 1 to 6. After 6 days of incubation, the cell cycle distributions were different because of the significant difference in the topography of each substrate. After incubation with CDDP at a concentration equal to the IC_{50} for each culture condition, CDDP showed a significant effect on the cell cycle of MDA-MB-231 cells as compared with that of control (without CDDP administration).

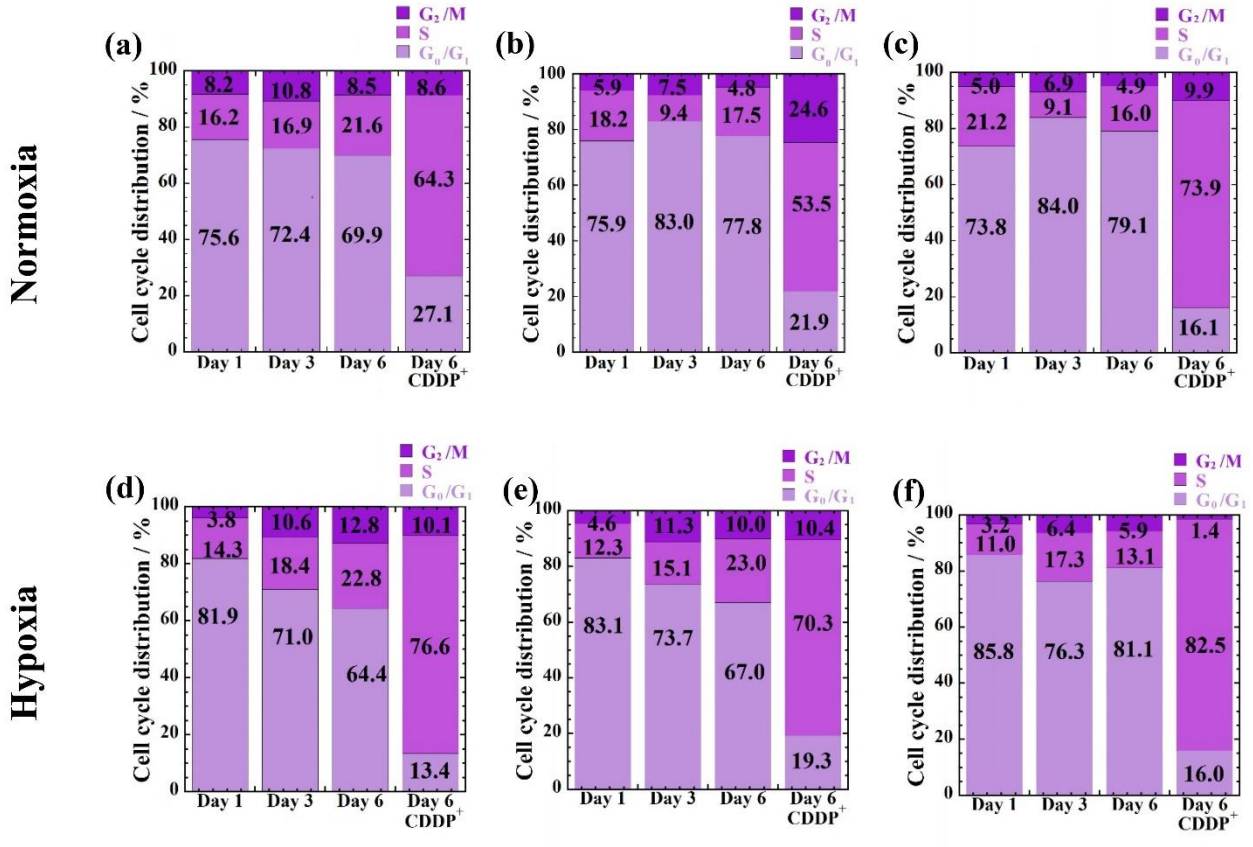

Figure 3 Effect of oxygen concentrations on the cell cycle distribution of MDA-MB-231 cells following incubation on PLLA substrates ((a, d) A-PLLA, (b, e) R-PLLA, and (c, f) F-PLLA) after without treatment (control), treated with CDDP at a concentration equal to IC_{50} for each culture condition in G_0/G_1 (light purple colors), S (purple colors), and G_2/M (dark purple colors) for 1 to 6 days.

For cells exposed to CDDP (IC_{50} value), the prolonged S phase following 3 days of incubation indicates the inhibition of DNA replication. In addition, a small increment in the fraction of cells in the S phase was observed following treatment with CDDP under hypoxia as compared to that under normoxia. This was due to the prolonged G_0/G_1 phase in hypoxia. In addition, EMT could

have been induced. However, EMT–cell cycle arrest has not been elucidated comprehensively in the literature.

3.4. PLLA Substrates Induced EMT

To study substrate-induced EMT, transforming growth factor *β* (TGF-β) [24, 25], snail family zinc finger 2 (SNAI2) [24, 26], and zinc finger E-box binding homeobox 1 (ZEB1) [24, 26] were analyzed. TGF-β can induce EMT and SNAI2 and ZEB1 are potent repressors of epithelial cell marker of E-cadherin (CDH1). Vimentin is a mesenchymal marker [24]. Cancer cells respond to the hypoxic microenvironment via hypoxia-inducible factor 1α (HIF-1α) [27, 28], which functions as an EMT promoter.

As the tumor progresses, the ECM is modified to create a considerably stiff and aligned architectural microenvironment. For example, under hypoxia, cells produced ECM with aligned collagen fibers, which affects cell morphology and mortality [29].

Figure 4, Figure 5 and Figure 6 show the expression of *HIF-1α*, *TGF-β*, *vimentin*, *CDH1*, *SNAI2*, and *ZEB1* genes in MDA-MB-231 cells cultured on three different types of substrates with and without subsequent treatment with CDDP at a concentration equal to IC_{50} for each culture condition for 6 days under both normoxic and hypoxic conditions. MDA-MB-231 cells incubated on PLLA substrates with CDDP treatment did not show a significant change in the expression of HIF-1α (Figure 4(a–a")).

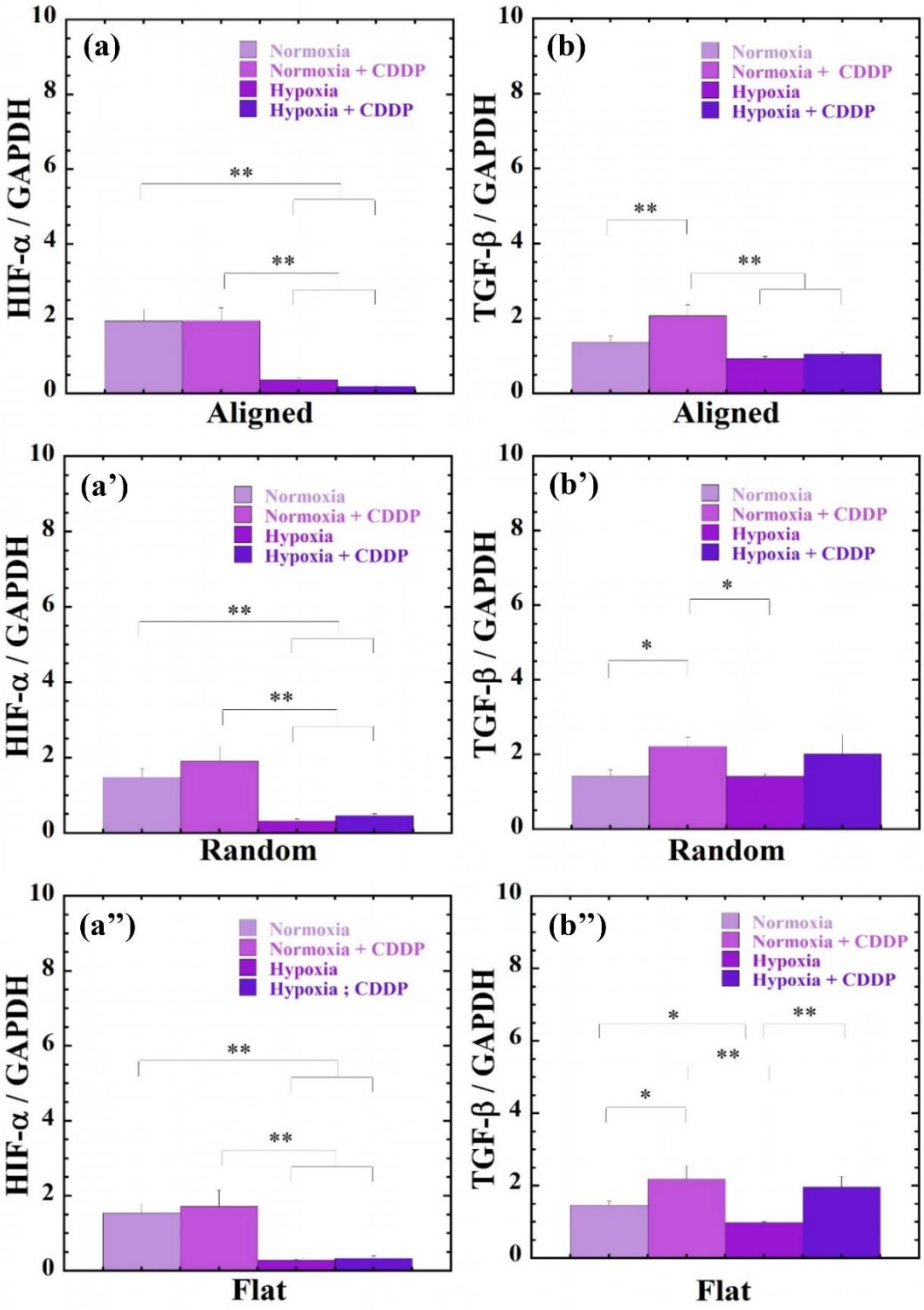

Figure 4 Effects of the topography of PLLA substrates and oxygen concentrations on the expression of *HIF-1α* (a–a") and *TGF-β* (b–b") genes in MDA-MB-231 cells incubated with and without CDDP at a concentration equal to IC_{50} for each culture condition. *$p < 0.05$ and **$p < 0.01$.

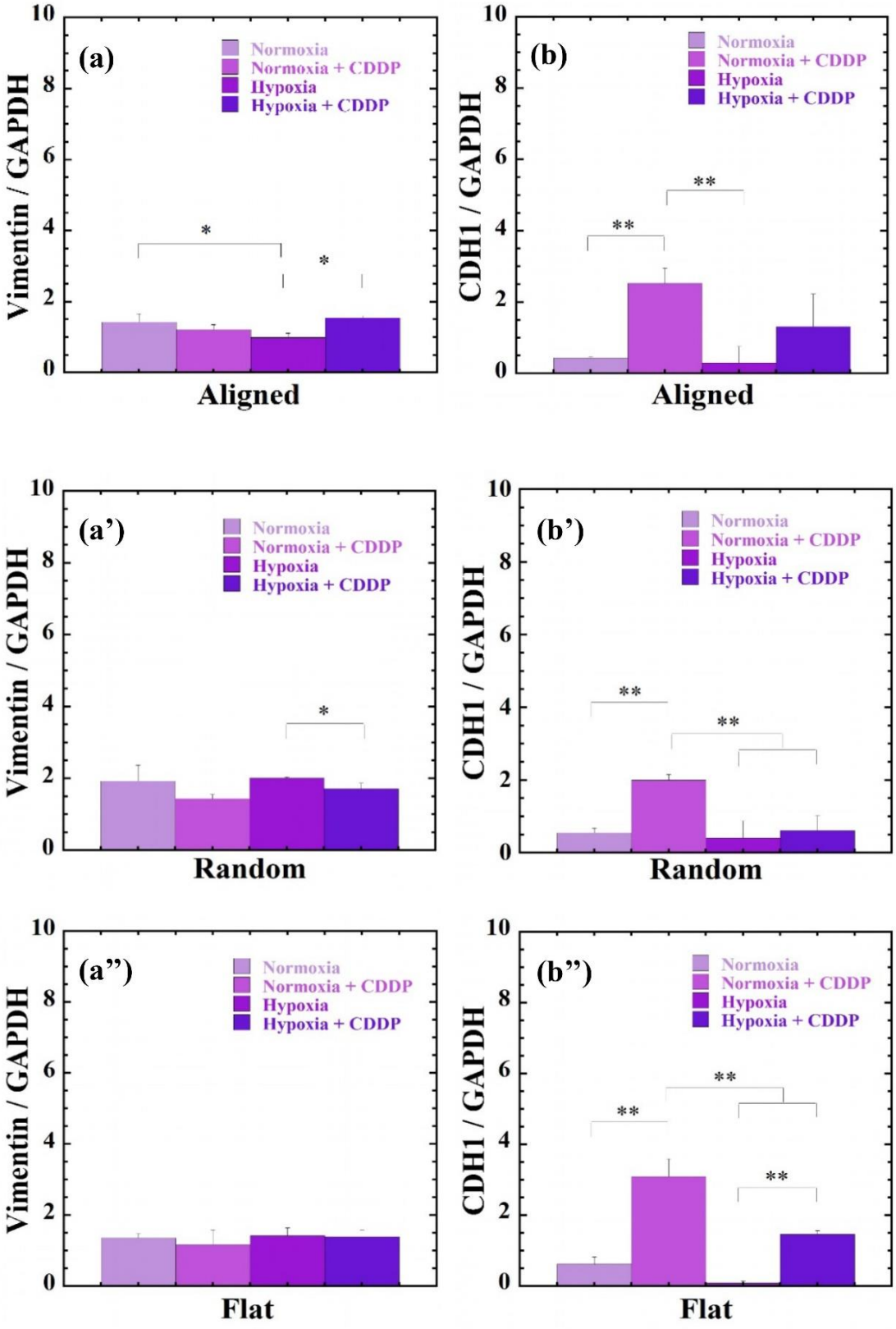

Figure 5 Effects of the topography of PLLA substrates and oxygen concentrations on the expression of *vimentin* (a–a") and *CDH1* (b–b") genes in MDA-MB-231 cells incubated with and without CDDP at a concentration equal to IC_{50} for each culture condition. *$p < 0.05$ and **$p < 0.01$.

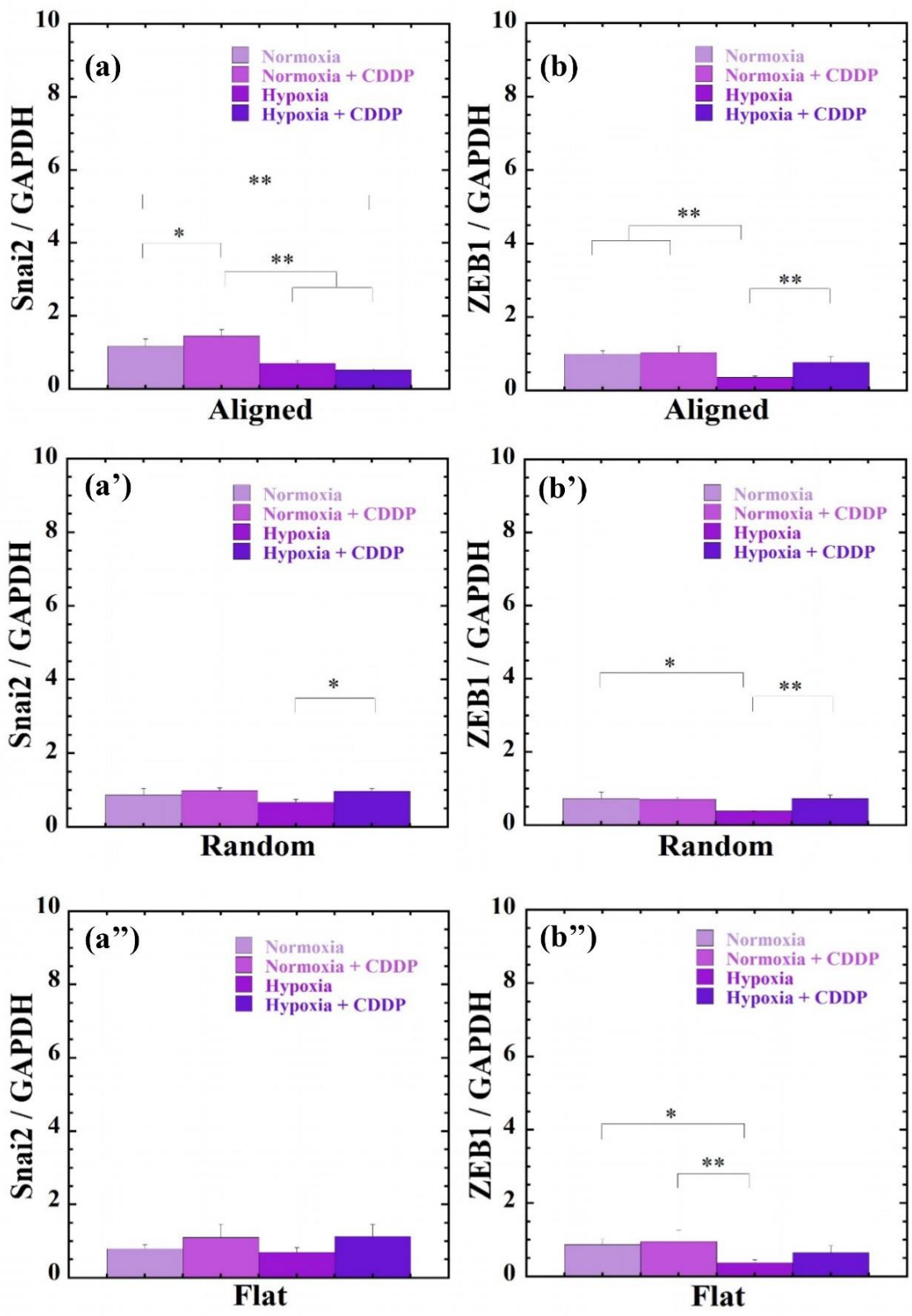

Figure 6 Effects of the topography of PLLA substrates and oxygen concentrations on the expression of *SNAI2* (a–a") and *ZEB1* (b–b") genes in MDA-MB-231 cells incubated with and without CDDP at a concentration equal to IC_{50} for each culture condition. *p < 0.05 and **p < 0.01.

Under hypoxic conditions, the levels of HIF-1α were significantly repressed in MDA-MB-231 cells culture on all PLLA substrates than under normoxic conditions, indicating that the cells underwent low oxygen environment due to slow adaptation to hypoxia. At the early stage of hypoxia, cytosolic levels of HIF-1α are low due to hydroxylation of HIF-1α by oxygen-sensing prolyl hydroxylase domain protein that targets HIF-1α for degradation via proteasome [28].

The TGF-β levels were markedly increased in MDA-MB-231 cells under normoxia when incubated on A-PLLA (1.4-fold) with CDDP than under normoxic without CDDP but not on A-PLLA substrate under hypoxia (Figure 4b). A similar result was obtained when the cells were incubated on R-PLLA (Figure 4b'). When incubated on F-PLLA, the CDDP treatment exerted a significant change in the expression of TGF-β under both normoxic and hypoxic conditions (Figure 4b").

Vimentin is expressed on the surface of MDA-MB-231 cells and differently on PLLA substrates (Figure 5(a–a")). The cells incubated under normoxia did not show a significant increase in the expression of vimentin, whereas its expression in cells incubated on A-PLLA with CDDP treatment under hypoxia was higher than in cells without CDDP treatment (control) on A-PLLA (Figure 5a). In contrast, the expression of vimentin was significantly repressed in cells incubated with R-PLLA and treated with CDDP under hypoxia than in cells without CDDP treatment (Figure 5a'). A-PLLA was found to be more effective in enhancing the expression of vimentin because of the synergetic effect of fiber alignment and stiffness. Stiffening and aligned EMC were observed in the vicinity of tumors [29].

The expression of CDH1 is shown in Figure 5(b–b"). For the expression of CDH1, changes similar to those shown in Figure 4(b–b") were observed in MDA-MB-231 cells on PLLA substrates. The behavior was consistent with the results obtained for the expression of TGF-β under both normoxic and hypoxic conditions. Significant repression of the expression of CDH1 was observed for MDA-MB-231 cell culture without CDDP treatment (control) on each PLLA substrate. This behavior was consistent with the results of a stiff substrate down-regulating the CDH1 expression [20].

The expression of SNAI2 increases in MDA-MB-231 cells incubated on A-PLLA under normoxia and R-PLLA under hypoxia following CDDP treatment (Figure 6(a, a")). Increased up-regulation of ZEB1 in the cells incubated on A-and R-PLLA substrates under hypoxia showed a trend to further induce EMT (Figure 6(b, b')). However, a statistical difference between normoxic and hypoxic conditions was observed. The expression was lower in the hypoxic environment than in the normoxic condition, indicating that EMT was less promoted in the hypoxic environment. The topographical effect on EMT could be more beneficial for the mesenchymal type of cells (such as MDA-MB-231).

Altogether, the obtained results imply that PLLA substrates do not cause a highly significant change in induction (transcription factors [SNAI2 and ZEB1] associated with EMT) and acquisition (vimentin expression) of EMT.

3.5. Linkage to CDH1 in Drug Susceptibility

The induction of EMT is believed to be an efficient anti-cancer drug-resistant mechanism for cancer cells. However, in each of the substrates tested in this study, the topographical effect on the expression of the *CDH1* gene was more beneficial for MDA-MB-231 cells under different oxygen concentrations, in which a significant level of up-regulation in CDH1 was evident for cells

incubated with CDDP treatment (Figure 5(b–b")). Our findings showed that the link between topography-mediated drug susceptibility of PLLA substrates and CDH1 suppression between normoxic and hypoxic conditions affected the anti-cancer drug resistance in cancer cells.

The ratio of IC_{50} values of three different PLLA substrates under different oxygen concentration levels was plotted as a function of relative values in CDH1 expression (Figure 7). The IC_{50} value under hypoxia was significantly enhanced with decreased *CDH1* expression accompanied by a robust correlation, as observed in the plot. This result suggests that the repression of CDH1 is the driving force of CDDP resistance in MDA-MB-231 cells. The CDDP treatment under hypoxia indicates poor adhesion of MDA-MB-231 cells as well as significant repression in CDH1.

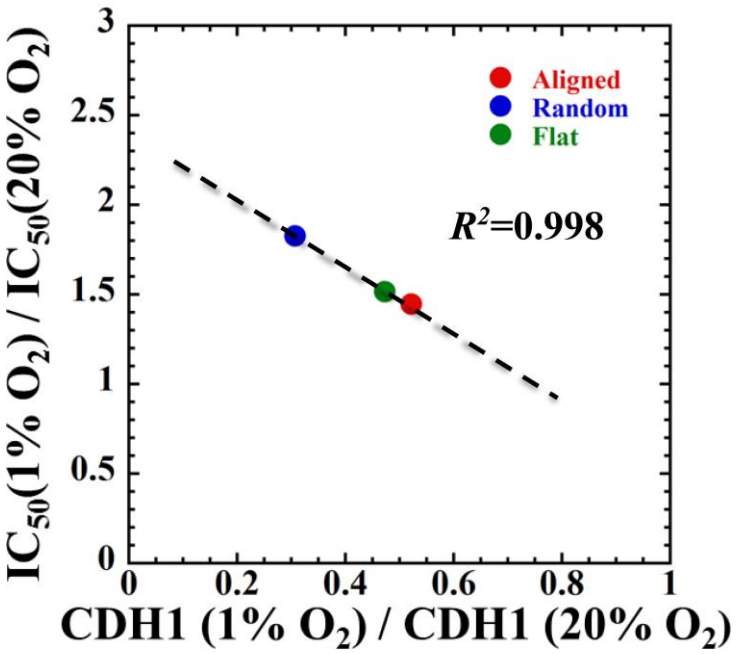

Figure 7 Relationships between the ratio of IC_{50} values of three PLLA substrates under different oxygen concentration levels and relative values in CDH1 expression. The dashed line derived by the least-squares method indicates linear regression.

For breast and colon cancer cells, collective cell migration through cell–cell junctions of the neighboring cells have been widely observed [30]. In collective cancer cell migration, groups of cancer cells migrate together, which could be a more efficient pathway for metastasis, perhaps with the integration of diverse cell populations or multicellular signals that spread to other organs [30]. The experimental evidence may point out the proposed scenario that CDDP treatment and cell–cell interactions can cause altered cell–cell binding, CDH1 expression, and drug susceptibility inhibiting the mass migration of cancer. These are challenging subjects to investigate in a future study.

4. Conclusions

A combination of surface topographies (fiber alignments) and different stiffness of PLLA substrates were used to evaluate the effects of surface topographies and stiffness of the substrate on the direct relationship between anti-cancer drug (CDDP) sensitivity in MDA-MB-231 cells and mesenchymal properties with induction of EMT under normoxic and hypoxic conditions.

MDA-MB-231 cells showed different IC_{50} values when they were cultured on different substrates and at different oxygen concentrations. Almost three-fold higher CDDP resistance was observed under hypoxia after incubation with A-PLLA as compared to that with R-PLLA under normoxia. For cells, PLLA substrates did not cause a significant change in induction and acquisition of the EMT, indicating the EMT exerted no effect on the drug susceptibility. Interestingly, the connection between the drug sensitivity and repression of CDH1 mediated by substrate surface topography had an implication for the anti-cancer drug resistance of MDA-MB-231 cells.

The present study has demonstrated the drug sensitivity and induction of the EMT induced by topographies of a variety of substrates. Cancer metastasis and anti-cancer drug susceptibility in biological phenomena are highly complex. Although the difficulty in the strategy lies in the interpretation of the local microenvironmental status of ECM in malignant tumor cells, anthropogenic substrates that mimic the *in vivo* microenvironment are expected to provide a novel approach for the development of new therapeutic strategies.

Acknowledgments

This work was supported by the TTI Grant (Special Research Project: FY2019-2021).

Author Contributions

Contributed to the initiating idea and performed most of the experiments: Sasaki R, Ito H and Okamoto M. Supervised research: Okamoto M. The manuscript was written through contributions of all authors.

Competing Interests

The authors have declared that no competing interests exist.

Additional Materials

The following additional materials are uploaded at the page of this paper.

1. Supplementary materials.
2. Figure S1: Platinum–DNA adducts. (a) monoadducts, (b) intrastrand crosslinks (1,2-d(GpG) (G: guanine), 1,2-d(ApG) (A: adenine), 1,3-d(GpXpGp), where there is another base (X) in between the two platinated guanines), (c) interstrand crosslinks (G-G), and (d) DNA-protein crosslinks.
3. Figure S2: FE-SEM images showing electrospun fiber substrates: (a) A-PLLA and (b) R-PLLA.
4. Table S1: Morphological parameters, tensile properties and degree of crystallinity of polymeric fiber-based substrates.

References

1. Health, Labour and Welfare Ministry. Table 7 deaths/mortality rates [Internet]. Tokyo: Ministry of Health Labour and Welfare; 2020 [cited date 2020 November 16]. Available from: http://www.mhlw.go.jp/toukei/saikin/hw/jinkou/geppo/nengai19/dl/h7.pdf.

2. Allemani C, Weir HK, Carreira H, Harewood R, Spika D, Wang XS, et al. Global surveillance of cancer survival 1995–2009: Analysis of individual data for 25 676 887 patients from 279 population-based registries in 67 countries (CONCORD-2). Lancet. 2015; 385: 977-1010.
3. Hanahan D, Weinberg RA. Hallmarks of cancer: The next generation. Cell. 2011; 144: 646-674.
4. Jin X, Mu P. Targeting breast cancer metastasis. Breast Cancer Basic Clin Res. 2015; 9: BCBCR-S25460.
5. Park CC, Bissell MJ, Barcellos Hoff MH. The influence of the microenvironment on the malignant phenotype. Mol Med Today. 2000; 6: 324-329.
6. Gikes DM, Semenza GL, Wirtz D. Hypoxia and the extracellular matrix: Drivers of tumour metastasis. Nat Rev Cancer. 2014; 14: 430-439.
7. Xiong GF, Xu R. Function of cancer cell-derived extracellular matrix in tumor progression. J Cancer Metastasis Treat. 2016; 2: 357-364.
8. Insua Rodriguez J, Oskarsson T. The extracellular matrix in breast cancer. Adv Drug Deliv Rev. 2016; 97: 41-55.
9. Lu P, Weaver VM, Werb Z. The extracellular matrix: A dynamic niche in cancer progression. J Cell Biol. 2012; 196: 395-406.
10. Humphrey JD, Dufresne ER, Schwartz MA. Mechanotransduction and extracellular matrix homeostasis. Nat Rev Mol Cell Bio. 2014; 15: 802-812.
11. Dalby MJ, Gadegaard N, Tare R, Andar A, Riehle MO, Herzyk P, et al. The control of human mesenchymal cell differentiation using nanoscale symmetry and disorder. Nat Mater. 2007; 6: 997-1003.
12. Fischbach C, Chen R, Matsumoto T, Schmelzle T, Brugge JS, Polverini PJ, et al. Engineering tumors with 3D scaffolds. Nat Methods. 2007; 4: 855-860.
13. Bray LJ, Binner M, Holzheu A, Friedrichs J, Freudenberg U, Hutmacher DW, et al. Multi-parametric hydrogels support 3D in vitro bioengineered microenvironment models of tumour angiogenesis. Biomaterials. 2015; 53: 609-620.
14. Zustiak S, Nossal R, Sackett DL. Multiwell stiffness assay for the study of cell responsiveness to cytotoxic drugs. Biotechnol Bioeng. 2014; 111: 396-403.
15. Schrader J, Gordon Walker TT, Aucott RL, van Deemter M, Quaas A, Walsh S, et al. Matrix stiffness modulates proliferation, chemotherapeutic response, and dormancy in hepatocellular carcinoma cells. Hepatology. 2011; 53: 1192-1205.
16. Nguyen TV, Sleiman M, Moriarty T, Herrick WG, Peyton SR. Sorafenib resistance and JNK signaling in carcinoma during extracellular matrix stiffening. Biomaterials. 2014; 35: 5749-5759.
17. Shin JW, Mooney DJ. Extracellular matrix stiffness causes systematic vatiations in proliferation and chemosensitivity in myeloid leukemias. Proc Natl Acad Sci Unit States Am. 2016; 113: 12126-12131.
18. Craene DB, Berx G. Regulatory networks defining EMT during cancer initiation and progression. Nat Rev Cancer. 2013; 13: 97-110.
19. Girard YK, Wang C, Ravi S, Howell MC, Mallela J, Alibrahim M, et al. A 3D fibrous scaffold inducing tumoroids: A platform for anticancer drug development. PloS ONE. 2013; 8: e75345.
20. Domura R, Sasaki R, Okamoto M, Hirano M, Kohda K, Napiwocki B, et al. Comprehensive study on cellular morphologies, proliferation, motility, and epithelial–mesenchymal transition of

breast cancer cells incubated on electrospun polymeric fiber substrates. J Mater Chem B. 2017; 5: 2588-2600.
21. Domura R, Sasaki R, Ishikawa Y, Okamoto M. Cellular morphology–mediated proliferation and drug sensitivity of breast cancer cells. J Funct Biomater. 2017; 8: 18.
22. Kinoshita M, Okamoto Y, Furuya M, Okamoto M. Biocomposites composed of natural rubber latex and cartilage tissue derived from human mesenchymal stem cell. Mater Today Chem. 2019; 12: 315-323.
23. Ishikawa Y, Sasaki R, Domura R, Okamoto M. Cellular morphologies, motility, and epithelial–mesenchymal transition of breast cancer cells incubated on viscoelastic gel substrates in hypoxia. Mater Today Chem. 2019; 13: 8-17.
24. Yilmaz M, Christofori G. EMT, the cytoskeleton, and cancer cell invasion. Cancer Metastasis Rev. 2009; 28: 15-33.
25. Zavadil J, Böttinger E. TGF-β and epithelial-to-mesenchymal transitions. Oncogene. 2005; 24: 5764-5774.
26. Peinado H, Olmeda D, Cano A. Snail, ZEB and bHLH factors in tumour progression: An alliance against the epithelial phenotype? Nat Rev Cancer. 2007; 7: 415-428.
27. Nelson MT, Short A, Cole L, Gross AC, Winter J, Eubank TD, et al. Preferential, enhanced breast cancer cell migration on biomimetic electrospun nanofiber 'cell highways'. BMC Cancer. 2014; 14: 825.
28. Brahimi Horn MC, Pouysségur J. Oxygen, a source of life and stress. FEBS Lett. 2007; 581: 3582-3591.
29. Riching KM, Cox BL, Salick MR, Pehlke C, Riching AS, Ponik SM, et al. 3D collagen alignment limits protrusions to enhance breast cancer cell persistence. Biophys J. 2014; 107: 2546-2558.
30. Clark AG, Vignjevic DM. Modes of cancer cell invasion and the role of the microenvironment. Curr Opin Cell Biol. 2015; 36: 13-22.